

Term-dependent lifetime broadening effect on the 4d photoelectron spectrum of atomic thulium

A G Kochur¹, I D Petrov¹, J Schulz² and Ph Wernet³

¹ Rostov State University of Transport Communication, 2 Narodnogo Opolcheniya, Rostov-na-Donu 344038, Russia

² Centre for Free-Electron Laser Science at DESY, D-22603 Hamburg, Germany

³ BESSY, Albert-Einstein-Str. 15, D-12489, Berlin, Germany

E-mail: agk@rgups.ru

Received 24 July 2008, in final form 16 September 2008

Published 23 October 2008

Online at stacks.iop.org/JPhysB/41/215002

Abstract

The 4d photoelectron spectrum of free thulium atoms is measured and calculated in the single-configuration intermediate-coupling approximation considering multiplet splitting and lifetime broadening of the spectral components due to radiationless transitions following the 4d ionization. The individual natural widths of the $4d^9 4f^{13}$ multiplet components are found to differ considerably, and the experimental profile of the spectrum can be reproduced theoretically only if this effect is taken into account.

1. Introduction

It is known that the 4d photoelectron spectra of the lanthanides with half- and less-than-half-filled 4f subshell have components with very different natural widths due to the fact that the very rapid 4d–4f4f super-Coster–Kronig (SCK) transitions are forbidden for the low-ionization-energy high-spin components of the $4d^9 4f^n$ multiplet [1–3]. A high-spin state $4d^9 4f^n ({}^{2S_{\max}+1}L)$ is the state where the spins of all the 4f electrons and the spin of the 4d vacancy are parallel thus giving the total spin $S_{\max} = n/2 + 1/2$. The 4d–4f4f transition would lead to the final state $4d^{10} 4f^{n-2} \varepsilon l$ where εl is a photoelectron. The maximal possible spin here is $n/2 - 1/2 < S_{\max}$, which means that the transition is forbidden. The natural widths of the high-spin $4d^9 4f^n ({}^{2S_{\max}+1}L)$ states are then very small as compared with those of other $4d^9 4f^n$ states for which the 4d–4f4f SCK transition is the dominant decay pathway. The calculations [1, 3] showed that the difference in individual widths of the $4d^9 4f^n (n \leq 7)$ multiplet components is huge, and taking this into account is indispensable in the theoretical description of the 4d spectra. The same situation is expected in the np photoelectron spectra of the nd transition elements ($n = 3, 4$) with half- and less-than-half filled nd subshells where the high-spin states $np^5 nd^n ({}^{2S_{\max}+1}L)$ cannot decay by the np – $ndnd$ SCK transition. This has been demonstrated in the cases of the 3p photoelectron spectra of atomic Mn [4] and Mn compounds [5].

As can easily be seen, if the 4f-subshell occupancy in lanthanides or the nd -subshell occupancy in the nd transition elements is greater than $2l + 1$ then the SCK transitions are not forbidden, and the differences in multiplet component widths are not expected to be dramatic. Nevertheless, it is understood that the individual component widths can be term dependent and considerably different even in those cases. This has been shown, for example, in the calculations of the $L\gamma$ emission spectra of Tm and Yb [6], $K\beta$ emission spectra of Fe, Co and Ni [7], and in 3p photoelectron spectra of the atomic Fe and Co [8], atomic Ni [9], and NiCl_2 [10]. No study on the term dependence of the natural widths in the 4d photoelectron spectra of more-than-half-filled 4f subshell lanthanides has yet been performed.

In this work, we report on the 4d photoelectron spectrum of atomic thulium. A theoretical description of the spectrum includes the calculation of the multiplet structure, photoionization cross sections and the broadening of each individual $4d^{-1}$ state due to all possible SCK, Coster–Kronig (CK) and Auger decays.

2. Experiment

A beam of free Tm atoms was produced using a resistively heated oven at approximately 840 °C [11]. The atoms were ionized by linearly polarized undulator radiation at the SX-700

monochromator of the BW3 undulator station at HASYLAB in Hamburg. [12]

The photoelectrons emerging from the interaction region were detected by a SCIENTA SES200 spherical electron analyser. The analyser only accepted electrons with an angle of emission close to the magic angle 54.7° relative to the polarization axis of the synchrotron radiation. The photoelectron spectra were recorded at a fixed pass energy of 300 eV while scanning the retarding lens voltage of the analyser. For more details of the experimental setup see [13].

The spectrum was taken at a photon energy of 502.5 eV with a total instrumental bandwidth of approximately 0.7 eV (full width at half maximum (FWHM)). The binding energies have been normalized with respect to the Tm 4f lines [14].

3. Method of calculation

3.1. Multiplet structure and photoionization cross sections

The $4d^{-1}$ multiplets and the 4d photoelectron spectra in rare earth atoms were systematically calculated by Demekhin *et al* using equal widths for all components [15]. They have shown that a good agreement with the experiment can be achieved even in the single-configuration approximation if the configuration interaction effect is accounted for by reducing the electrostatic interaction integrals. The scaling of the interaction integrals accounts for the pressing down of the multiplet components coming from their interaction with higher-lying excited configurations. In this work, we employ the single-configuration intermediate coupling approximation with a scaling factor of 0.67 for 4d–4f and 4f–4f interaction integrals. The scaling factor was optimized to get the best agreement of the calculated spectrum with the experiment. The radial parts of atomic orbitals and the spin–orbit constants are calculated in the Pauli–Fock approximation [16].

The ground state of the Tm atom is the lower N_5 component of the N_{45} spin doublet, $4d^{10}4f^{13}2F_{7/2}$. The final states of the core after photoabsorption are described in the intermediate-coupling approximation as the expansions over the basic states with the same total momentum J :

$$|EJ\rangle = \sum_i \langle 4d^9 4f^{13} \beta_i L_i S_i J | EJ \rangle |4d^9 4f^{13} \beta_i L_i S_i J\rangle. \quad (1)$$

Here β_i is an additional quantum number distinguishing between the states with the same $L_i S_i$ but different genealogy. The energies E and the decomposition coefficients $\langle 4d^9 4f^{13} \beta_i L_i S_i J | EJ \rangle$ were determined by numerical diagonalization of the secular equation matrices. The only empirical parameter entering our calculation of the final-state multiplet structure is the scaling factor for the interaction integrals discussed above.

By employing the methods of [17, 18] the cross section of the photoabsorption processes

$$4d^{10}4f^{13}2F_{7/2} + h\nu \rightarrow 4d^9 4f^{13} EJ + \varepsilon l \quad (2)$$

can be expressed in the form of the product

$$\sigma^{\varepsilon l}(2F_{7/2} \rightarrow EJ) = \frac{4\pi^2 \alpha a_0^2 h\nu}{15} (2J+1) B(EJ) \times [(I \| C^{(1)} \| d) \langle \varepsilon l | r | 4d \rangle]^2. \quad (3)$$

Here $l = \{p, f\}$ is the photoelectron orbital momentum quantum number, α is the fine structure constant, a_0 is the Bohr radius, $h\nu$ is the absorbed photon energy, $(I \| C^{(1)} \| d)$ is the reduced matrix element as defined in [17], and

$$\langle \varepsilon l | r | 4d \rangle = \int_0^\infty P_{\varepsilon l}(r) r P_{4d}(r) dr \quad (4)$$

is the radial dipole transition integral.

The term B depends on the structure of the final state of the core (1) and is independent of the photoelectron angular momentum.

We found that the radial integrals (4) do not change significantly within the energy range of interest, so they were taken constant. The total cross section for each $4d^9 4f^{13} EJ$ multiplet component was calculated by summing up the partial 4d– εp and 4d– εf cross sections.

3.2. Component widths

Consider the decay of the $4d^9 4f^{13} (EJ)$ state into the state $4d^{10} n_1 l_1^{-1} n_2 l_2^{-1} (E'J') \varepsilon l$ through 4d– $n_1 l_1 n_2 l_2$ radiationless transition, εl being Auger, CK or SCK continuous spectrum electron. We consider every possible combination of $n_1 l_1, n_2 l_2 = \{4f, 5s, 5p, 6s\}$. Both $4d^9 4f^{13} (EJ)$ and $4d^{10} n_1 l_1^{-1} n_2 l_2^{-1} (E'J')$ states are expressed as expansions like (1). Then the width of the transition between those two particular terms is

$$\Gamma_{4d-n_1 l_1 n_2 l_2} (EJ - E'J') = 2\pi \sum_l \left| \sum_i \sum_j C_i C_j A_{ij}^{\varepsilon l} (4d - n_1 l_1 n_2 l_2) \right|^2, \quad (5)$$

where $C_i = \langle 4d^9 4f^{13} \beta_i L_i S_i J | EJ \rangle$ and $C_j = \langle 4d^{10} n_1 l_1^{-1} n_2 l_2^{-1} \beta_j L_j S_j J' | E'J' \rangle$ are the decomposition coefficients, and $A_{ij}^{\varepsilon l}$ is the amplitude of the radiationless transition between the basic LSJ states with the ejection of an εl electron into the continuum. General expressions for the amplitudes $A_{ij}^{\varepsilon l}$ are given in [19].

Partial width of the $4d^9 4f^{13} (EJ)$ state due to the 4d– $n_1 l_1 n_2 l_2$ transition is the sum of (5) over the final-state core terms:

$$\Gamma_{4d-n_1 l_1 n_2 l_2} (EJ) = \sum_{E'J'} \Gamma_{4d-n_1 l_1 n_2 l_2} (EJ - E'J'). \quad (6)$$

The total $4d^9 4f^{13} (EJ)$ component width is the sum of (6) over all possible SCK, CK and Auger transitions:

$$\Gamma(EJ) = \sum_{n_1 l_1, n_2 l_2} \Gamma_{4d-n_1 l_1 n_2 l_2} (EJ). \quad (7)$$

One may also introduce the partial mean width of the Tm N_5 level,

$$\Gamma_{4d-n_1 l_1 n_2 l_2} (N_5) = \sum_{EJ} \frac{2J+1}{g(4d^9 4f^{13})} \Gamma_{4d-n_1 l_1 n_2 l_2} (EJ), \quad (8)$$

and the total mean width of the N_5 level,

$$\Gamma(N_5) = \sum_{n_1 l_1, n_2 l_2} \Gamma_{4d-n_1 l_1 n_2 l_2} (N_5). \quad (9)$$

In (8), $g(4d^9 4f^{13}) = 140$ is the statistical weight of the configuration.

Table 1. Calculated ionization energies of the Tm $4d^9 4f^{13} EJ$ states (IE), cross sections of their production via photoionization of the Tm $4d^{10} 4f^{13} {}^2F_{7/2}$ state (σ), their partial SCK and CK ($\Gamma_{4d-n_1l_1n_2l_2}$) and total (Γ) widths.

IE , eV	Dominant basic state ^a	$\sigma(EJ)$, arbitrary units	$\Gamma_{4d-n_1l_1n_2l_2}(EJ)$, eV				$\Gamma(EJ)$, eV
			4d–4f4f	4d–4f5s	4d–4f5p	4d–4f6s	
197.99	0.823 1P_1	0.017	4.782	0.323	0.773	0.032	5.939
197.45	0.957 1H_5	0.614	6.116	0.460	1.114	0.046	7.766
195.79	0.689 3G_3	0.040	5.999	0.394	0.961	0.039	7.423
193.72	0.769 3P_2	0.380	4.943	0.314	0.755	0.031	6.074
192.74	–0.626 3D_3	0.441	5.546	0.363	0.877	0.036	6.851
191.91	0.910 3G_4	0.582	5.976	0.381	0.933	0.037	7.357
191.80	0.582 3F_2	0.005	4.529	0.286	0.681	0.028	5.554
188.83	0.799 3D_1	0.166	5.070	0.343	0.817	0.033	2.549
188.35	0.872 3H_4	0.015	2.008	0.146	0.351	0.014	6.293
187.10	1.000 3P_0	0	4.757	0.230	0.704	0.028	5.809
187.00	0.912 3P_1	0.048	4.835	0.301	0.727	0.029	5.922
186.76	0.674 1F_3	0.477	5.558	0.373	0.900	0.037	6.898
186.63	0.936 3G_5	0.834	6.247	0.404	0.989	0.040	7.711
185.90	0.617 3D_2	0.117	4.718	0.302	0.722	0.029	5.801
183.50	0.912 3F_3	0.119	4.121	0.257	0.622	0.025	5.055
183.25	–0.677 3F_4	0.150	3.791	0.240	0.586	0.023	4.670
182.75	0.946 3H_5	0.244	2.143	0.160	0.384	0.015	2.733
182.44	0.737 1D_2	0.268	4.286	0.262	0.622	0.025	5.226
180.12	0.730 1G_4	0.637	3.322	0.207	0.508	0.020	4.087
179.22	1.000 3H_6	1.000	1.627	0.128	0.305	0.012	2.103

^a Principal term in the expansion (1).

The expressions for the amplitudes $A_{ij}^{\epsilon l}(4d - n_1l_1n_2l_2)$ in (5) contain the electrostatic interaction integrals $R^k(n_1l_1n_2l_2, 4d\epsilon l)$. They were calculated with the core orbitals of the initial configuration $4d^{-1}$. The continuous spectrum wavefunctions ϵl were calculated in the Pauli–Fock approximation in configuration–average potentials of respective final-state two-vacancy configurations built with the core functions of the initial-state configuration $4d^{-1}$. The continuous spectrum electron energies ϵ were taken constant within the same $4d-n_1l_1n_2l_2$ transition. The integrals $R^k(n_1l_1n_2l_2, 4d\epsilon l)$ were not scaled.

4. Results and discussion

Experimental and theoretical Tm 4d photoelectron spectra are presented in figure 1(a). The experimental spectrum is shown with open circles. It is shifted along the vertical axis; its zero intensity level is marked with the horizontal lines. The bar spectrum represents the calculated photoionization cross sections. The profiles of the theoretical spectra were calculated as the sums of the Lorentzians with areas equal to calculated cross sections, and the FWHM equal to calculated components natural widths. The profiles thus obtained were then convoluted with the Gaussians of FWHM = 0.7 eV to account for the experimental broadening. The theoretical profiles were calculated in two ways: (1) with accurate accounting for the individual component natural widths (solid line) and (2) with equal mean natural widths for all the components (dashed line). Calculated natural widths of the spectral components are shown in figure 1(b) and listed in the last column of table 1.

Table 2. Mean partial widths ($\Gamma_{4d-n_1l_1n_2l_2}(N_5)$), and total mean width ($\Gamma(N_5)$) of the Tm N_5 level.

Transition	$\Gamma_{4d-n_1l_1n_2l_2}(N_5)$, eV
4d–4f4f	4.3311
4d–4f5s	0.2887
4d–4f5p	0.6985
4d–4f6s	0.0281
4d–5s5s	0.0037
4d–5s5p	0.0132
4d–5s6s	0.0005
4d–5p5p	0.0124
4d–5p6s	0.0006
4d–6s6s	0.00001
$\Gamma(N_5)$, eV	5.3768

Table 1 lists the calculated ionization energies of the Tm $4d^9 4f^{13} EJ$ states, the cross sections of their production via photoionization of the Tm $4d^{10} 4f^{13} {}^2F_{7/2}$ state, and their partial SCK and CK widths. The assignment of the $4d^9 4f^{13}$ multiplet components is given in column 2 of table 1 where the dominant terms in the expansions (1) are listed.

The partial component widths due to the N_5OO , N_5OP and N_5PP Auger transitions are the same for each component, and they coincide with partial N_5 level widths (8). The partial N_5 level widths due to all possible radiationless decays and the total mean width of the Tm N_5 level are listed in table 2.

It is seen from table 2 that the SCK and CK transitions are responsible for 99.4% of the total width. Both SCK and CK partial widths are term dependent, and this determines the term dependence of the total widths of the components. One can see from table 1 and figure 1(b) that the individual component

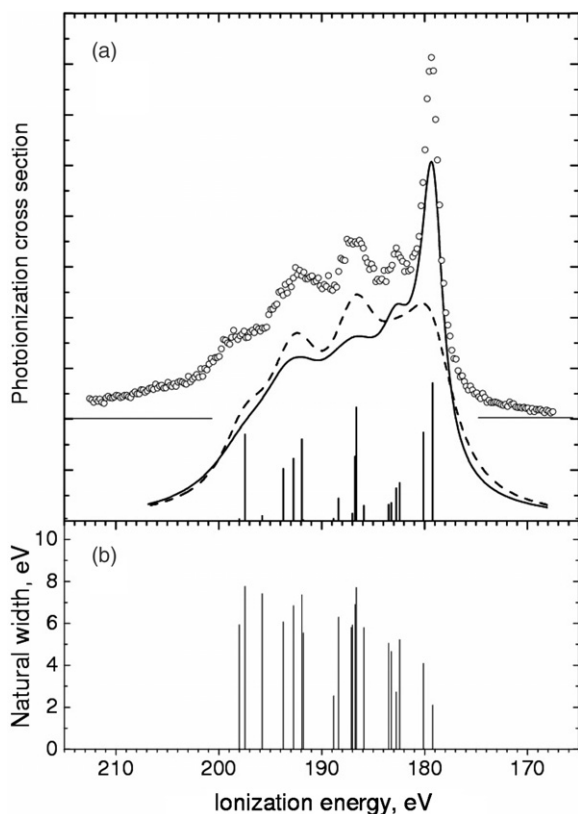


Figure 1. (a) Experimental and calculated 4d photoionization spectrum of atomic thulium. Circles: experiment; bars: calculated photoionization cross sections; solid line: theoretical spectrum with individual components natural widths; dashed line: theoretical spectrum with equal mean components widths. (b) Calculated component natural widths. Assignment of components is given in table 1.

widths differ significantly—up to a factor of 3.7. Evidently, this is a circumstance that cannot be ignored in the theoretical description of any phenomenon dealing with the 4d-hole states in Tm.

The theoretical spectrum calculated with individual component widths (the solid line in figure 1(a)) is in good agreement with the experiment. A broad low-intensity shoulder in the experimental spectrum at about 206 eV which is not reproduced by the calculation comes from the photoionization processes accompanied by satellite shake excitations as discussed in [3].

The spectrum calculated with the same total mean N_5 level width of 5.38 eV for each component (the dashed line in figure 1(a)) cannot reproduce the profile of the experimental spectrum. We performed the equal-component-width calculations taking component widths both greater and less than the calculated one and were never able to get an agreement with the experiment.

5. Conclusion

The term dependence of the $4d^{-1}$ states' natural widths is great even in lanthanides with more-than-half-filled 4f subshell. This must be taken into account in the theoretical description of the 4d photoelectron spectra of those elements as well as in any phenomena having to do with the 4d vacancies.

References

- [1] Ogasawara H, Kotani A and Thole B T 1994 *Phys. Rev. B* **50** 12332–41
- [2] Kochur A G, Sukhorukov V L and Petrov I D 1996 *J. Phys. B: At. Mol. Opt. Phys.* **39** 4565–72
- [3] Gerth Ch, Godehusen K, Richter M, Zimmermann P, Schulz J, Wernet Ph, Sonntag B, Kochur A G and Petrov I D 2000 *Phys. Rev. A* **61** 022713
- [4] von dem Borne A, Johnson R L, Sonntag B, Talkenberg M, Verweyen A, Wernet Ph and Schulz J 2000 *Phys. Rev. A* **62** 052703
- [5] Tagushi M, Uozumi T and Kotani A 1997 *J. Phys. Soc. Japan* **66** 247–56
- [6] Demekhin V F, Sukhorukov V L, Yavna V A, Kulagina S A, Prosandeev S A and Bairachnyi Yu I 1976 *Bull. Acad. Sci. USSR Phys. Ser.* **40** 28–34 translated from 1976 *Izvestiya Akademii Nauk SSSR, Seriya Fizicheskaya, USSR* **40** 255–62
- [7] Nemoshkalenko V V, Demekhin V F, Krivitsky V P, Nosachev Yu F, Petrov I D, Yavna V A and Yavna S A 1985 *VINITI (USSR)* No 3840–85
- [8] Tiedtke K, Gerth Ch, Martins M and Zimmermann P 2001 *Phys. Rev. A* **64** 022705
- [9] Tiedtke K, Gerth Ch, Kanngießner B, Obst B, Zimmermann P, Martins M and Tutay A 1999 *Phys. Rev. A* **60** 3008–12
- [10] Okada K, Kotani A, Ogasawara H, Seno Y and Thole D T 2003 *Phys. Rev. B* **47** 6203–6
- [11] Ross K and Sonntag B 1995 *Rev. Sci. Instrum.* **66** 4409–33
- [12] Björneholm O, Federmann F, Larsson C, Hahn U, Rieck A, Kakar S, Möller T, Beutler A and Fössing F 1995 *Rev. Sci. Instrum.* **66** 1732–4
- [13] Wernet Ph, Schulz J, Sonntag B, Godehusen K, Zimmermann P, Grum-Grzhimailo A N, Kabachnik N M and Martins M 2001 *Phys. Rev. A* **64** 042707
- [14] Wernet Ph, Verweyen A, Schulz J, Sonntag B, Godehusen K, Müller R, Zimmermann P and Martins M 2002 *J. Phys. B: At. Mol. Opt. Phys.* **35** 3887–900
- [15] Demekhin V F, Yavna S A, Bairachnyi Yu and Sukhorukov V L 1977 *J. Struct. Chem.* **18** 513–19 translated from 1977 *Zhurnal Strukturnoi Khimii (USSR)* **18** 644
- [16] Kau R, Petrov I D, Sukhorukov V L and Hotop H 1992 *Z. Phys. D* **39** 262
- [17] Yutsis A P, Levinson I B and Vanagas V V 1960 *Mathematical Apparatus of the Angular Momentum Theory* (Vilnius: State Publishing House for Political and Scientific Literature of Lithuanian SSR) p 244
- [18] Lindgren I and Morrison J 1982 *Atomic Many-Body Theory (Springer Series in Chemical Physics vol 13)* (Berlin: Springer) p 469
- [19] Kochur A G, Dudenko A I and Petrov I D 2004 *J. Phys. B: At. Mol. Opt. Phys.* **37** 2401–9